Measurement of ^{238}U spallation product cross sections at 1 GeV per nucleon

J. TAIEB[a,c], P. ARMBRUSTER[a], J. BENLLIURE[b] , M. BERNAS[c], A. BOUDARD[d], S. CZAJKOWSKI[e], T. ENQVIST[a], F. REJMUND[c], R. LEGRAIN[d], S. LERAY[d], B. MUSTAPHA[c], M. PRAVIKOFF[e], K.-H. SCHMIDT[a], C. STEPHAN[c], L. TASSAN-GOT[c], C. VOLANT[d], W. WLAZLO[f]

[a] GSI, Planckstr. 1, 64291 Darmstadt, Germany

[b] Univ. de Santiago de Compostela, E-15706 Santiago de Compostela, Spain

[c] IPN, Centre Scientifique, F-91406 Orsay CEDEX, France

[d] DAPNIA/SPhN, CEA Saclay, F-91191 Gif/Yvette CEDEX, France

[e] CENBG, F-33175 Gradignan CEDEX, France

[f] Jagiellonian University, Institute of Physics, ul. Reymonta 4, 30-059 Krakow, Poland

Abstract

Spallation residues produced by the interaction of 1·A GeV ^{238}U ions with a proton target have been measured using the FRagment Separator (FRS) of GSI. The use of the reverse kinematics allows a determination of isotopic cross sections before all beta decays and most of the alpha decays. Production cross section for more than 500 isotopes have been obtained with very high accuracy. Mean value and standard deviations of the velocity distribution for every fragment have also been measured. Comparisons to a code and to a parameterization are also presented.

I. Introduction

The study of the spallation reaction with heavy nuclei got a renewed interest these last years thanks to various types of projects namely the so-called Accelerator Driven Systems[1,2] (ADS), the

neutron sources based on spallation reactions and the radioactive-beam facilities[3]. The spallation of uranium is more specifically the privileged reaction for the production of Radioactive Ion Beams in ISOL-type facilities[4]. The knowledge of the production yields of ^{238}U spallation residues seems to be of very high interest on the applied level. On the fundamental side, the production of spallation residues is strongly conditioned by the fission of isotopes during the evaporation phase. The measurement of such products gives therefore hints on the neutron-over-fission width (Γn/Γf) ratio and on the viscosity of nuclear matter.

For all those reasons, several experimental studies on the production spallation products of uranium have already been performed for nearly 45 years[5]. However, most results deal with fission products[6,7], which could be measured with quite good accuracy thanks to their high recoil velocity resulting from the fission process. As far as heavy evaporation residues are concerned, very few data are available. They have always been obtained by radio-chemical methods and are therefore most of the time cumulative and very partial[8]. The present study will concentrate on those evaporation residues.

II. Experiment

The main characteristic of the experiment carried out at GSI in July 1997 lies in the use of reverse kinematics at relativistic energies leading to strong forward focusing of the reaction products.

The 1·A GeV ^{238}U beam, produced by the synchrotron SIS of GSI, interacts with a liquid hydrogen target[9]. The products of the spallation reaction are then separated and analyzed by the spectrometer FRS[10]. Figure 1 gives an overview on the experimental apparatus. A more detailed description of the device is available in other publications[11,12].

It is worth noting that the FRS allows a full analysis and identification (Z, A, and velocity) of all produced fragments in two steps. The first magnetic selection mainly enables the rejection of the primary beam. The fragments are then slowed down in a thick passive energy degrader situated on the intermediate focal plane. The ions are finally subject to a second magnetic selection. Time-of-flight and horizontal position are measured by two plastic-scintillation detectors placed at the intermediate and final image planes. Two segmented ionization chamber[13] located at the very end of the spectrometer give energy-loss signals. Two sets of multi-wire proportional chambers supply the horizontal position and angle at the final focal plane.

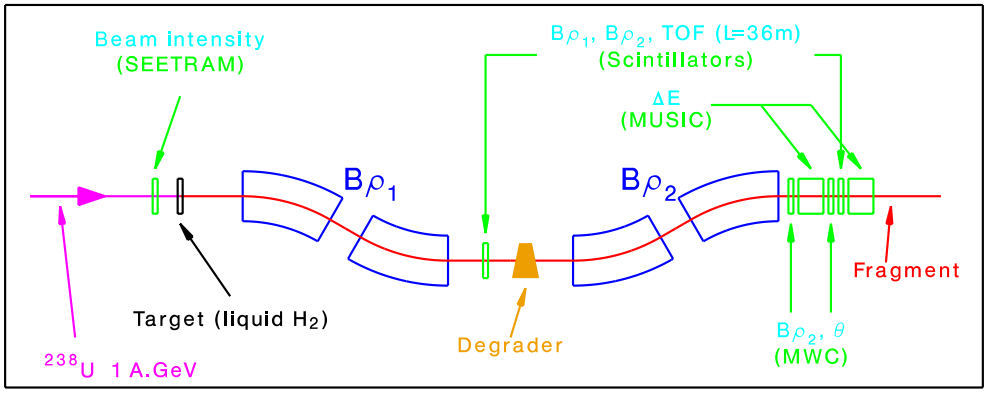

Figure 1. schematic view of the FRS

III. Data analysis

The combination of magnetic fields and position measurements at both image planes delivers the magnetic rigidity ($B\rho$) in both sections of the FRS. Combining $B\rho$ and time-of-flight measurements in the second stage (index 2) we deduce the ratio mass number (A) over ionic charge (q).

$$\left(\frac{A}{q}\right)_2 = \frac{e\times(B\rho)_2}{m_0\times c\times\beta_2\times\gamma_2} \qquad (1)$$

The reduced velocity (β_2) and the Lorenz factor (γ_2) are determined from time-of-flight, e is the electron charge, m_0, the atomic mass unit.

The energy of the ions amounts to 980·A MeV in the first stage and 700·A MeV in the second one. Consequently, most of the fragments are bare. As shown below, we will only consider ions, which are fully stripped all along the trajectory; therefore

$$\left(\frac{A}{q}\right)_2 = \left(\frac{A}{Z}\right)_2 \qquad (2)$$

The nuclear charge of the produced fragments is obtained from energy-loss measurements. Two ionization chambers[13] give two ΔE signals, which are combined in order to get a better resolution. This signal is correlated to a second energy-loss measurement deduced from the difference of magnetic rigidities before and after the degrader. Figure 2 shows a typical correlation of both quoted quantities.

Three different diagonals are to be seen. The central and most intense one refers to ions, which are bare in both sections of the separator. We only consider such ions in the analysis. The two other diagonals refer to other charge states. A weak background is produced by nuclear reactions in the energy degrader. Each spot of the central diagonal corresponds to one nuclear charge. The gate drawn on figure 2 matches with bismuth isotopes. This clearly demonstrates the high quality of the nuclear-charge separation and the complete rejection of non-bare isotopes.

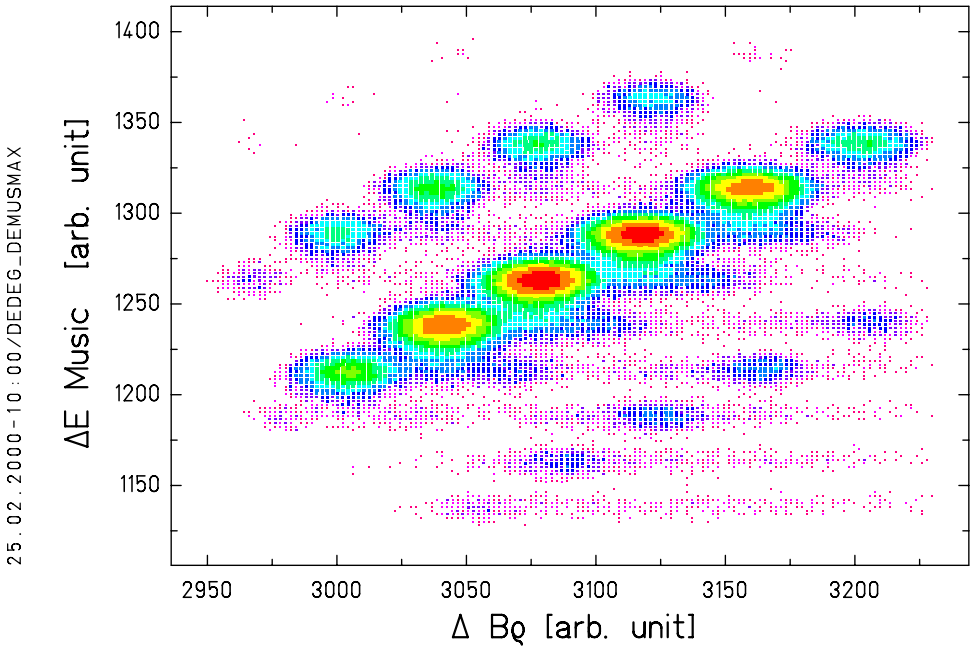

Figure 2. Charge resolution

The mass spectrum is obtained from equations (1) and (2) using the previously described nuclear-charge selection. We disentangle the various masses on a 2-dimensional plot, correlating the mass and the position at the intermediate focal plane. This way we avoid the broadening of the resolution due to aberrations. The obtained mass resolution ($A/\Delta A_{FWHM}$=300) is excellent and is mainly limited by the time-of-flight resolution (135 ps FWHM). Figure 3 shows a typical mass spectrum for bismuth isotopes. It is to be seen that most fragments are not fully transmitted in one setting. Therefore about 80 tunings of the spectrometer were carried out and combined for covering the whole range of produced isotopes.

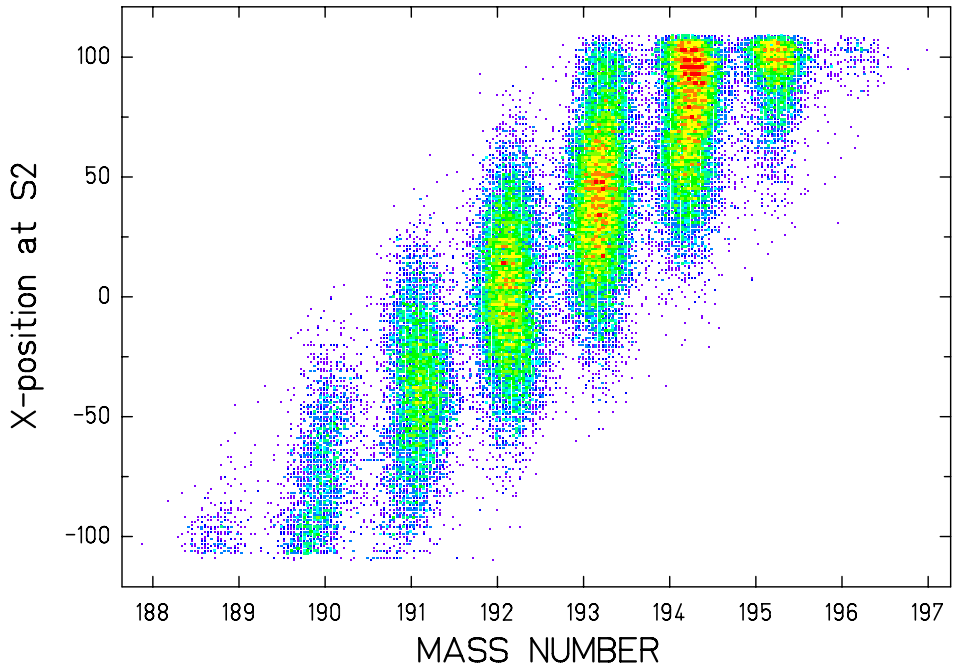

Figure 3. Mass resolution

The number of analyzed isotopes amounts to 500, covering almost all produced isotopes ranging from 50 to 0.01 mbarn. Only few nuclides with magnetic rigidities very close to that of the projectile could not be measured.

The data are corrected for losses due to charge states not considered in the analysis, only bare nuclei having been processed. That correction was estimated from atomic-physics codes[14] validated by numerous measurements, and ranges from 35% for uranium isotopes to less than 10% for thulium. We also take into account losses due to nuclear interactions in the various layers of matter in the intermediate image plane. That correction is estimated by a parameterization of nucleus-nucleus interaction cross-sections[15] and amounts to about 40%.

III. Results

Figure 4 shows preliminary isotopic cross sections for all elements ranging from uranium (Z=92) to thulium (Z=69). The error bars are still relatively high (40%). The reason is that all corrections have not been carefully performed yet. The final uncertainty should be in the order of 15%.

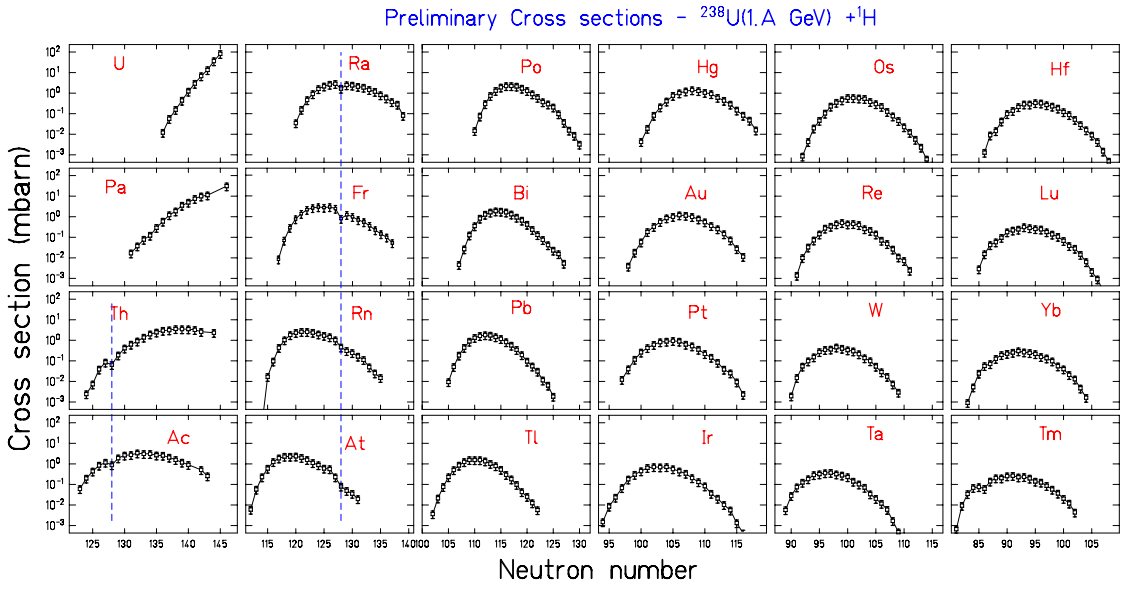

Figure 4. Isotopic distributions of all elements from uranium to thulium

Cross sections are obtained by normalizing the number of measured ions to the thickness of the target, which was precisely scanned during a previous experiment[11], and to the intensity of the beam monitored by the secondary-electron detector positioned upstream the target. Contributions of the target windows are also extracted from measurements with a fake empty target. That contribution is rather low for most fragments.

The shape of the isotopic distributions evolves from a very asymmetric one close to the projectile to a bell-shaped one about ten charges far from it. All distributions are very smooth except for neutron number equal to 128 where a slight dip can be seen and for very light fragments where the corrections need to be improved. The N=128 isotones suffer a very fast alpha decay onto the 126-neutron shell. The typical period is in the order of 200 ns whereas the time of flight of the ions is about 150 ns (eigentime). Since also isomeric states are populated with unknown probability, it is rather difficult to correct for that effect. When the decay period is even faster as it is the case for ^{215}Fr, there is a non-negligible chance that the decay occurs within the target, and the ion is "seen" as a daughter nucleus. Consequently, isotopes at the 126-neutron shell are in some cases over-produced (^{211}At or ^{210}Po for instance).

The same collaboration measured the production of gold spallation residues in 1996. The effect of the fission process along the evaporation process is nicely seen by comparing the production of isotopes of the projectile (uranium and gold). Figure 5 shows the production cross section as a function of the number of neutrons lost in both cases. The production of neutron-deficient isotopes is so strongly influenced by fission that only 10 isotopes of the projectile could be

analyzed in the uranium case, while 21 isotopes of gold were measured during the previous experiment.

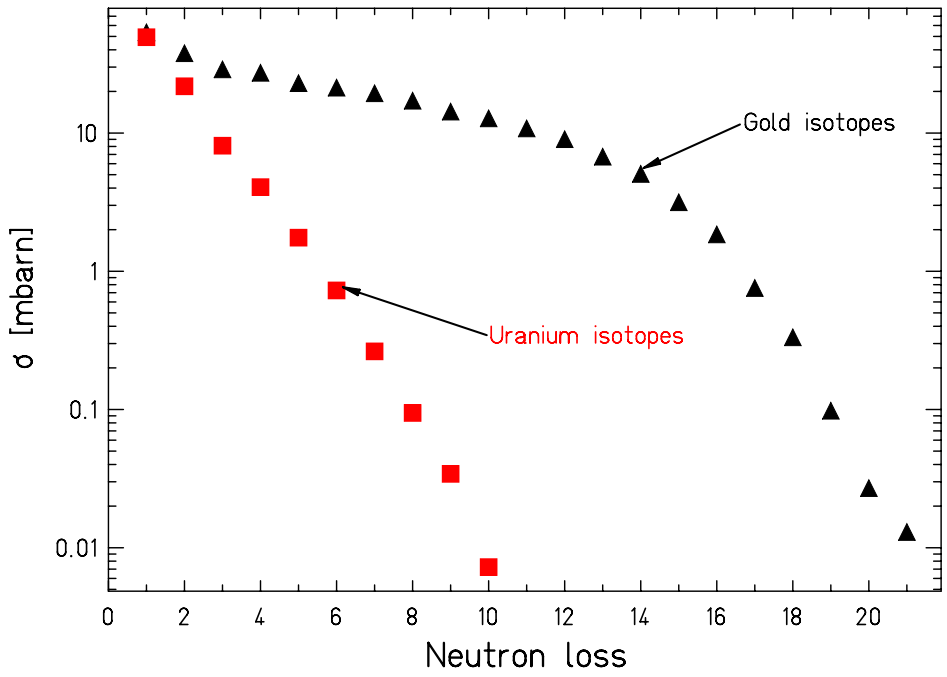

Figure 5. Comparison of the production of projectile isotopes in gold and uranium experiments

IV. Comparison to code and parameterization

Several parameterizations are available for estimating the production cross sections due to nuclear fragmentation. The EPAX formula[16] is one of the more common one. Unfortunately, most of them suppose that the limiting-fragmentation regime is reached, and they are therefore not energy dependent. Such parameterizations are not applicable for spallation reactions below 3 GeV in direct kinematics (or 3·A GeV in reverse kinematics). Silberberg, Tsao and Barghouty[17] proposed another formula dedicated to spallation reactions at lower energy, which considers the energy dependence.

Some Monte-Carlo codes also exist which try to reproduce the physical process by coupling an intra-nuclear cascade code (INC) to an evaporation model. The INC code ISABEL[18] coupled to the modern evaporation code ABLA[19] developed at GSI, called ISABLA, is able to nicely reproduce the production of evaporation residues in the spallation of gold.

Figure 6 shows the comparison of the data and the predictions of Silberberg, Tsao and Barghouty as well as the ISABLA code for 4 different nuclear charges, uranium, francium (Z=87), lead (Z=82), and iridium (Z=77). The parameterization gives a reasonable description of the data close to the projectile, for the lighter charges the distribution is too sharp, and the exponential decrease on the neutron-rich side does not fit the data. It is worth noting that the good agreement observed between data and parameterization for isotopes of uranium is not representative for the general behavior since the calculation exhibits the same slope for isotopes of the projectile in case of spallation of gold for instance. We saw in the previous section that the production of isotopes of the projectile in the gold and in the uranium cases are strongly different. Moreover, far from projectile (lead and iridium) the distributions proposed by the parameterization are getting shifted, certainly due to the lack of data in that mass-loss region.

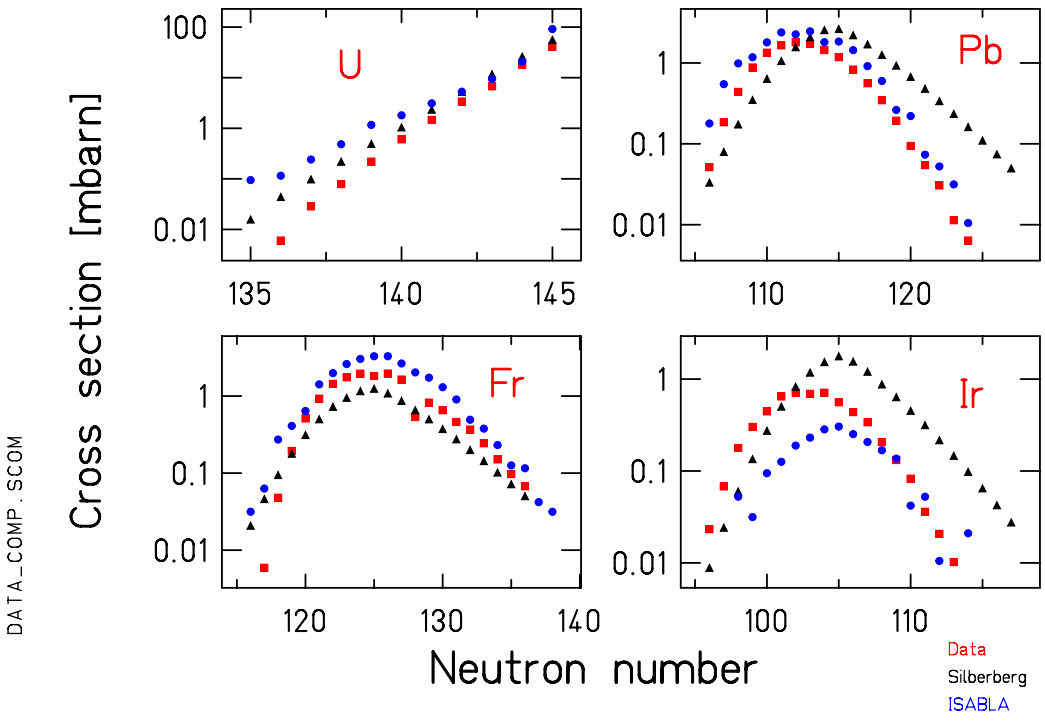

Figure 6. Isotopic distributions for uranium, francium, lead and iridium ; squares (resp. dots and triangles) represent the data (resp. ISABLA and parameterization)

ISABLA gives an overall better agreement than the parameterization. The height and the shape of the distribution are better reproduced except for the lightest shown charge where the simulated distribution is also shifted and for the lightest uranium isotopes, which are overestimated by ISABLA. The reason for that might be the absence of the treatment of light charged particles besides protons and alphas in the evaporation code ABLA.

V. Velocity distributions

After complete identification, we deduce the longitudinal velocity of the fragments from the measurement of the magnetic rigidity in the first part of the separator. Previous publications[11,12] detail the procedure and have already shown that we access the mean recoil velocity due to the nuclear reaction and the standard deviation of the Gaussian-like velocity distribution for every isotopes.

Figure 7 shows the standard deviation of the velocity distribution as a function of the mass loss for the uranium experiment in comparison with the gold experiment and the prediction of the Goldhaber model[20] and the Morrissey systematic[21]. The Goldhaber model is applied with a Fermi momentum equal to 265 MeV/c.

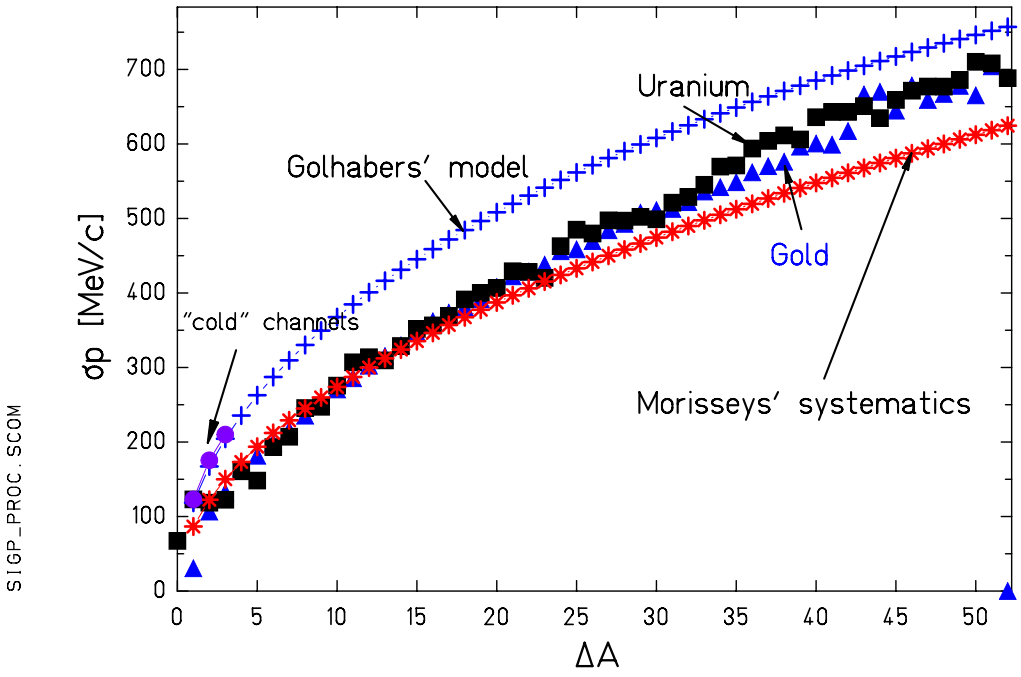

Figure 7. Comparison of the standard deviations obtained experimentally and predicted by model and systematic (see text for explanation)

The results obtained from the gold and uranium experiments are rather close one to the other for low and high mass losses and follow nicely the semi-empirical systematic of Morrissey for mass losses less than 20 units and then slowly reach values predicted by Goldhaber.

We specifically treated cold processes, namely the three first proton-removal channels (full dots in figure 7) which are only populated by purely abrasive peripheral reactions. In such collisions, only protons are kicked out of the uranium ion; the remnant is left with very low excitation energy, and therefore no evaporation is allowed. In such specific cases we show that the Goldhaber model succeeds nicely in estimating the broadening of the velocity distribution. Such phenomenon has already been observed in other experiments[22,23]. When the excitation energy is low, the broadening due to evaporation is much less for a given mass loss. When the excitation energy is high, the mean kinetic energy of the evaporated particles gets higher and the broadening gets closer to what is predicted by Goldhaber.

VI. Conclusion

The evaporation residues produced in spallation reactions of ^{238}U by protons have been measured in reverse kinematics at a beam energy of 1·A GeV. More than 500 isotopes have been fully identified (nuclear charge, atomic mass and recoil velocity) before every type of radioactive decay in far most cases. Neither code nor parameterization are nowadays able to reproduce the data with high accuracy as it could be done for previous experiment with less fissile isotopes (gold and lead).

Standard deviations of the velocity distributions have also been analyzed showing a good agreement with the Morrissey systematic and an apparently less good agreement with the Goldhaber model. When purely abrasive processes are selected (1, 2 and 3 proton-removal channels), the Goldhaber model succeeds in reproducing the data.

The authors are indebted to K. H. Behr, A. Brünle and K. Burkhard for technical support during the experiment

References

[1] C.D. Bowman Ann. Rev. Nucl. Part. Sci. 48 (1998) 505-556

[2] C. Rubbia et al. CERN Report CERN-LHC 96-011-ETT

[3] M. de Jong, C. Böckstiegel et al. Nucl. Phys. A 616 (1997) 363c

[4] G.S. Bauer, T. Broome et al. "ESS, a Next Generation Neutron Source for Europe", Vol III, The ESS technical study, ESS 96-53-M (1996), ISBN 90 237 6 659

[5] M. Lindner, R. N. Osborne Phys. Rev. 103,2 (1956) 378

[6] L. N. Andronenko, L. A. Vaishnene et al. Yad.Fiz. 24, 671 (1976); Sov.J.Nucl.Phys. 24, 354 (1976)

[7] J. K. P. Lee, G. Pilar, B. L. Tracy, L. Yaffe, J. Inorg. Nucl. Chem. 37 (1975) 2035-38

[8] Y. E. Titarenko, Y. E. Shvedov et al. 3rd International Conference on Accelerator Driven Transmutation Technologies and Applications, Praga June 1999

[9] P. Chesny, A. Forgeas et al. GSI Ann. Rep. 97-1 (1996) 190

[10] H. Geissel, P. Armbruster Nucl. Instr. and Meth.. A 364 (1992) 150

[11] B. Mustapha PhD thesis IPN Orsay (France) 1999

[12] F. Rejmund. et al., submitted to Nucl. Phys. A.

[13] W. B. Christie, J. L. Romero et al. Nucl. Instr. and Meth. A 255 (1987) 466-476

[14] C. Scheidenberger, Th Stölker et al. Nucl. Instr. and Meth. B 142 (1998) 441-462

[15] C. J. Benesh, B. C. Cook, J. P. Vary. Phys. Rev C 40 (1989) 1198-1206

[16] K. Suemmerer, B. Blank. Phys. Rev. C 61 (2000) 034 607

[17] R. Silberberg, C. H. Tsao, A. F. Barghouty, Astrophys. J. 501, 911 (1998)

[18] Y. Yariv, Z. Fraenkel. Phys. Rev. C 24 (1981) 488-94

[19] J. Benlliure et al. Nucl. Phys. A 628 (1998) 458

[20] A. S. Goldhaber. Phys. Lett. B 53 (1974) 306-8

[21] D. J. Morrissey Phys. Rev. C 39 (1989) 460-70

[22] E. Hanelt, A. Grewe et al. Z. Phys. A 346 (1993) 43-46

[23] K.-H. Schmidt, K. Sümmerer et al. Nucl. Phys. A542 (1992) 699-714